

# 12

## Application of Chemical Graph Theory for the Estimation of the Dielectric Constant of Polyimides

B. JEFFREY SHERMAN and  
VASSILIOS GALIATSATOS

### 12.1. INTRODUCTION

In recent years high-performance polymers have become important in the electronics industry as encapsulants for electronic components, interlayer dielectrics, and printed wiring board materials. The dielectric properties of the materials used in plastic packaging play an important role in device performance. Both the dielectric constant (or permittivity)  $\epsilon'$  (sometimes the symbol  $\epsilon$  is used) and the loss (or dissipation) factor  $\epsilon''$  influence the signal-carrying capacity and propagation speed of the device. Materials with low dielectric constants and low loss factors provide better device performance, as they allow faster signal propagation with less attenuation. The signal speed is the velocity of the electromagnetic radiation in the transmitting medium, which is inversely proportional to the square root of the dielectric constant of the material.

The ability to estimate accurately the dielectric properties of a polymer is of value in the development of new materials for use in the electronics industry. The purpose of this chapter is to report on calculations that estimate the dielectric constant of polymers that are sufficiently novel that their dielectric properties of

---

B. JEFFREY SHERMAN • Maurice Morton Institute of Polymer Science, University of Akron, Akron, Ohio 44325-3909. VASSILIOS GALIATSATOS • Maurice Morton Institute of Polymer Science, University of Akron, Akron, Ohio 44325-3909. Present Address: Huntsman Polymers Corporation, Odessa, Texas 79766.

*Fluoropolymers 2: Properties*, edited by Hougham *et al.* Plenum Press, New York, 1999.

interest are not yet tabulated in the usual handbooks. The ultimate goal of such predictive methodologies is the reduction of product development time and optimization of product performance.

The chapter is divided into the following sections. First, a brief introduction to group contribution methods is given with a major emphasis on the concept and limitations of this technique. An introduction to the use of chemical graph theory and how it applies to polymers and in particular to the dielectric constant is given next. Application of the method to a number of polyimides is then demonstrated and predictions are compared to experimental results.

## 12.2. QUANTITATIVE STRUCTURE–PROPERTY RELATIONSHIPS BASED ON GROUP CONTRIBUTION METHODS

Methods based on quantitative structure–property relationships (QSPR) have been available for some time now and have become more or less standard empirical techniques since the appearance in the literature of van Krevelen's now classic book currently in its third edition.<sup>1</sup> All these methodologies take advantage of the vast databases of experimental data that have been accumulated over the years by mainly industrial but also by academic laboratories. The methodology described by van Krevelen is based on group contribution methods and it works satisfactorily for those polymers for which information on group contributions exists.

However, if not enough experimental data are available to allow a robust statistical correlation, it is not possible to rely on group contribution methods. van Krevelen subsequently published an extensive, very useful review article on the power and limitations of group contribution methods.<sup>2</sup>

Briefly, in the QSPR methodology a repeat unit is separated into smaller chemical groups. Properties then are expressed as sums of group contributions from all the fragments that make up the structure. Group contributions are found by fitting the observed values of the properties of interest to experimental data on other polymers whose repeat unit contains the same types of groups. The properties of interest themselves are expressed as regression relationships in terms of the group contributions.

Dielectric constant and cohesive energy density are determined by the same type of electrical force. Based on that observation van Krevelen reported that values of  $\epsilon$  at room temperature (RT) correlate with the solubility parameter  $\delta$ :

$$(1) \quad \epsilon_{RT} \approx \delta_{RT}^2/7$$

For nonpolar polymers it is well known that the dielectric constant is directly related to the refractive index  $n$ :

$$(2) \quad \varepsilon = n^2$$

The dielectric constant is also directly related to the electrical resistivity  $R$

$$(3) \quad \log R = 23 - 2\varepsilon$$

It is also related to the cohesive energy density  $E_{\text{coh}}$ :

$$(4) \quad \varepsilon = 1/7(E_{\text{coh}})^{1/2}$$

Another, sometimes useful, equation is

$$(5) \quad \varepsilon_{\text{RT}} = (V_{\text{RT}} + 2P_{\text{LL}})/(V_{\text{RT}} - P_{\text{LL}})$$

where  $P_{\text{LL}}$  is the molar polarization,  $V$  is the molar volume, and the subscript RT again denotes room temperature.

### 12.3. APPLICATION OF CHEMICAL GRAPH THEORY TO QSPR

Chemical graph theory is based on the observation that the connectivity of a molecule is correlated to many of its intrinsic physical properties. Chemical graph theory has been successful in providing an estimate of the intrinsic properties of various low-molecular-weight compounds when employed together with a regression analysis.<sup>3,4</sup>

More recently Bicerano has presented a new methodology in which many physical properties are expressed in terms of connectivity indexes.<sup>5</sup> This method allows the prediction of properties for a large number of polymers. Instead of group contributions the methodology relies on summation of additive contributions over atoms and bonds.

Bicerano's method is based on the use of connectivity indexes, a concept first generated in graph theory. Graph theory has also been very useful in the development of algorithms for the prediction of structure and properties of elastomeric polymer networks.<sup>6-10</sup> Graph theoretical algorithms allow the dissection of the topological features of all the components in polymer networks. Elastically active chains, defects, loops of any size, and sol fraction analysis are all amenable to analysis by graph theory.

Connectivity indexes in particular may be used easily because each index can be calculated from valence bond diagrams. These indexes can also be correlated

with the physical properties of interest. Application of connectivity indexes has been successful in the past for molecules with well-defined chemical structures and a fixed number of atoms.<sup>11,12</sup>

Two basic quantities are the atomic simple connectivity index  $\delta$  and the atomic valence connectivity index  $\delta^v$ . These values are tabulated in Bicerano's book<sup>5</sup> (p. 17) for 11 chemical elements, namely: C, N, O, F, Si, P, S, Se, Cl, Br, and I. Values of  $\delta$  and  $\delta^v$  are also reported for various hybridizations (*sp*, *sp*<sup>2</sup>, etc.).  $\delta$  is equal to the number of nonhydrogen atoms to which a given atom is bonded.  $\delta^v$  is calculated through:

$$(6) \quad \delta^v \equiv (Z^v - N_H)/(Z - Z^v - 1)$$

where  $Z^v$  is the number of valence electrons of the atom,  $N_H$  is the number of hydrogens connected to that atom, and  $Z$  is the atom's atomic number.

Four types of indexes can be identified: path-labeled, cluster-labeled, path/cluster, and chain-labeled, denoted, respectively, by  ${}^m\chi_p$ ,  ${}^m\chi_c$ ,  ${}^m\chi_{p/c}$ , and  ${}^m\chi_{ch}$ . All calculations reported here are based on the zeroth- and first-order connectivity indexes,  ${}^0\chi$ ,  ${}^0\chi^v$  and  ${}^1\chi$ ,  ${}^1\chi^v$ , respectively, for the entire repeat unit and these are defined as:

$$(7) \quad {}^0\chi \equiv \sum_{\text{all-vertices}} (1/\delta^{1/2})$$

and

$$(8) \quad {}^0\chi^v \equiv \sum_{\text{all-vertices}} [1/(\delta^v)^{1/2}]$$

while

$$(9) \quad {}^1\chi \equiv \sum_{\text{all-vertices}} (1/\beta^{1/2})$$

and

$$(10) \quad {}^1\chi^v \equiv \sum_{\text{all-vertices}} [1/(\beta^v)^{1/2}]$$

with the bond indexes  $\beta$  and  $\beta^v$  being defined for each bond not involving a hydrogen atom. They are given as

$$(11) \quad \beta_{ij} \equiv \delta_i \cdot \delta_j$$

and

$$(12) \quad \beta_{ij}^v \equiv \delta_i^v \cdot \delta_j^v$$

Use of connectivity indexes has been reported by Polak and Sundahl, who give two expressions for the polarizability of aliphatic polymers and for polymers containing ether and carbonyl groups.<sup>13</sup> The expression for the aliphatic polymers is

$$(13) \quad P = 8.86 {}^0\chi_p - 8.85\chi_{p/c} - 21.49$$

where  ${}^0\chi_p$  is the zero-order path index and  ${}^4\chi_{p/c}$  is the fourth-order path/cluster index. The equation that addresses polymers that contain ether and carbonyl groups is

$$(14) \quad P = 7.39 {}^0\chi_p - 4.72 \chi_{p/c} - 14.47$$

Polak and Sundahl used the Clausius–Mossotti equation to combine molar volume and polarizability to obtain values of dielectric constant.

## 12.4. PREDICTION OF DIELECTRIC CONSTANT

The basic regression equation for the dielectric constant employed for the polymers cited in this text is

$$(15) \quad \varepsilon_{RT} = 1.412014 + (0.00188E_{\text{coh}_1} + N_{dc})/V_w$$

where

$$(16) \quad N_{dc} = 19N_N + 7N_{\text{backbone(O,S)}} + 12N_{\text{side group(O,S)}} + 52N_{\text{sulfone}} - 2N_F \\ + 8N_{\text{Cl,Br(asym)}} + 20N_{\text{Si}} - 14N_{\text{cyc}}$$

Equation (15) has a standard deviation of 0.0871 and a correlation coefficient of 0.979. It is based on a data set containing 61 polymers chosen in such a way as to avoid incorporation of the effects of additives and fillers. Further analysis of the data set gave the following results:

- Fedors-type<sup>14</sup> cohesive energy  $E_{\text{coh}}$  correlated best with dielectric constant.
- Cohesive energy density  $E_{\text{coh}}/V$ , van der Waals volume  $V_w$ , and  $[E_{\text{coh}} + N_{dc}/c]$  all improved the correlation significantly, where  $c$  (in this case equal to 0.00188) is a fitting parameter and  $N_{dc}$  is defined by Eq. (16).

The symbols in Eq. (16) are as follows:

- $N_N$  is the number of nitrogen atoms in the repeat unit.
- $19N_N$  is a correction term that accounts for the underestimation of the nitrogen-containing groups in the original data set.

- $7N_{\text{backbone(O, S)}}$  and  $12N_{\text{sidegroup(O, S)}}$  are the contribution of the total number of oxygen and (divalent only) sulfur atoms in the main chain and in side groups, respectively.
- $52N_{\text{sulfone}}$  is the contribution from all sulfur atoms in the highest oxidation state only.
- $2N_{\text{F}}$  represents the (negative) contribution from fluorine atoms.
- $8N_{\text{Cl,Br(asym)}}$  represents the number of chlorine and bromine atoms attached to the chain asymmetrically.
- $20N_{\text{Si}}$  represents the contribution of silicon atoms.
- $14N_{\text{cyc}}$  is the contribution from nonaromatic rings containing no double bonds.

$E_{\text{coh}}$  is calculated by employing the following equations:

$$(17) \quad E_{\text{coh}} = 9882.5 \cdot \chi + 358.7(6N_{\text{atomic}} + 5N_{\text{group}})$$

with

$$(18) \quad N_{\text{atomic}} = 4N_{\text{S}} + 12N_{\text{sulfone}} - N_{\text{F}} + 3N_{\text{Cl}} + 5N_{\text{Br}} + 7N_{\text{cyanide}}$$

and

$$\begin{aligned} N_{\text{group}} \equiv & 12N_{\text{hydroxyl}} + 12N_{\text{amide}} + 2N_{\text{nonamide(NH)unit}} - N_{\text{(alkylether-O-)}} - N_{\text{C=C}} \\ & + 4N_{\text{nonamide-(C=O)-next to H}} + 7N_{\text{-(C=O)-in carboxylic acid, ketone, aldehyde}} \\ & + 2N_{\text{other-(C=O)}} + 4N_{\text{nitrogen atoms in six-membered aromatic ring}} \end{aligned}$$

$N_{\text{atomic}}$  is dependent on the total number of atoms of given types, with electronic configurations specified by appropriate pairs of atomic indexes. The terms on the right-hand side of Eq. (18) not been defined earlier are as follows:

- $N_{\text{cyanide}}$  is the number of nitrogen atoms with  $\delta = 1$  and  $\delta^v = 5$ .
- $N_{\text{group}}$  is, like  $N_{\text{dc}}$  above, a correction factor that improves the statistical correlation. Its terms are as follows:  $N_{\text{hydroxyl}}$  is the number of OH groups in alcohols and phenols. Contributions from OH groups in carboxylic or sulfonic acid groups are not incorporated in this term.
- $N_{\text{amide}}$  is the total number of amide groups in the repeat unit.
- $N_{\text{nonamide(NH)unit}}$  is the contribution from the NH units in those polymers where there is no carbonyl group adjacent to NH. NH units encountered in urethane groups are also included in this category.

- $N_{(\text{nonamide } \text{-(C=O)- next-to-H)}}$  is the number of carbonyl groups next to a nitrogen atom that does not have any attached hydrogens. Carbonyl groups in urethane units are part of this contribution.
- $N_{\text{-(C=O)- in-carboxylic-acid, ketone, aldehyde}}$  is the total number of carbonyl groups in carboxylic acid, ketone, and aldehyde.
- $N_{\text{other-(C=O)-}}$  is the number of C=O groups in ester and carbonate moieties as well as in anhydride groups.
- $N_{(\text{alkyl-ether-O-})}$  is the number of ether linkages between two units both of which are connected to the oxygen atom via an alpha carbon atom.
- $N_{\text{C=C}}$  is the number of carbon-carbon double bonds.
- $N_{\text{nitrogen-atoms-in-six-membered-aromatic-ring}}$  is the number of nitrogen atoms in six-membered aromatic rings.

The van der Waals volume  $V_w$  was calculated according to the following two equations:

$$(20) \quad V_w = 2.286940 \cdot {}^0\chi + 17.140570 \cdot {}^1\chi^v + 1.369231 \cdot N_{\text{vdw}}$$

and

$$(21) \quad N_{\text{vdw}} = N_{\text{methyl, nonaromatic}} + 0.52N_{\text{methyl, aromatic}} + N_{\text{amide, nonaromatic}} + N_{\text{OH}} \\ + N_{\text{cyanide}} - 3N_{\text{carbonate}} - 4N_{\text{cyc}} - 2.5N_{\text{fused}} + 7N_{\text{Si}} + 8N_{\text{S}} - 4N_{\text{Br}}$$

$N_{\text{vdw}}$  is a correction term that improves the correlation by compensation for the under/over estimation of the various group contributions. The terms in the right-hand side of the equation not defined earlier are as follows:

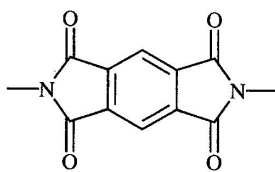
- $N_{\text{methyl-nonaromatic}}$  is the number of methyl groups connected to nonaromatic atoms.
- $N_{\text{methyl-aromatic}}$  is the number of methyl groups attached to aromatic atoms.
- $N_{\text{amide-nonaromatic}}$  is the number of linkages between amide groups and nonaromatic atoms.
- $N_{\text{cyanide}}$  and  $N_{\text{carbonate}}$  are the number of CN and OCOO groups, respectively.
- $N_{\text{fused}}$  is the number of rings in “fused” rings. However “fused” in this case does not have the same definition as in organic chemistry.
- $N_{\text{Si}}$ ,  $N_{\text{S}}$ , and  $N_{\text{Br}}$  are the numbers of silicon, divalent sulfur, and bromine atoms, respectively.

## 12.5. CALCULATIONS AND COMPARISON WITH EXPERIMENT

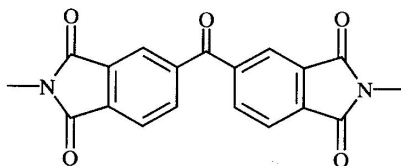
Calculations of connectivity indexes and subsequent dielectric constant predictions were accomplished by using Molecular Simulations Inc. Synthia polymer module running under the Insight II interface on a Silicon Graphics Crimson workstation. All calculations were performed on the polymer's repeat unit, which was first energy-minimized through a molecular-mechanics-based algorithm.

Experimental values were obtained from a number of sources.<sup>15-18</sup> Table 12.1 identifies the structure of repeat units of all the polyimides mentioned in this work. Table 12.2 gives experimental data for dielectric constants obtained with dry

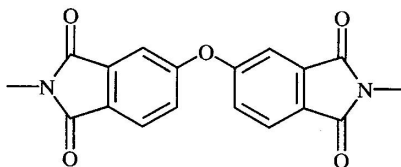
Table 12.1. Identification of Polyimide Repeat Units



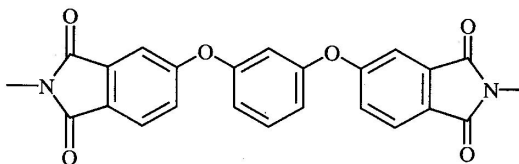
PMDA—Pyromellitic dianhydride



BTDA—Benzophenone tetracarboxylic dianhydride

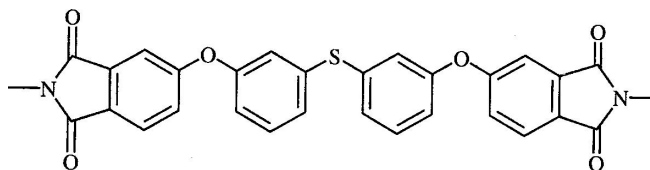


ODPA—4,4'-oxydipthalic anhydride

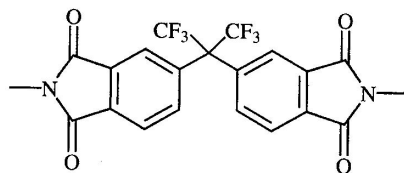


HQDEA—1,4'-bis(3,6dicarbpxyphenoxy) benzene dianhydride

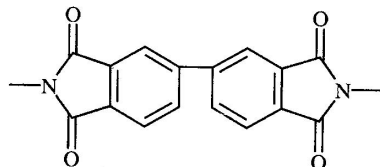




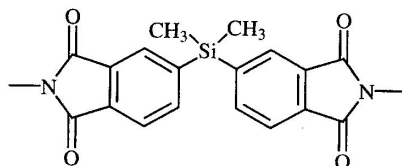
BDSDA—4,4'-bis(3,4-dicarboxyphenoxy) diphenylsulfide dianhydride



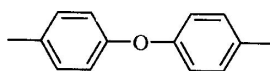
6FDA—2,2'-bis(3,4-dicarboxy phenyl) hexafluoropropane dianhydride



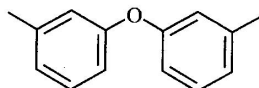
BPDA—3,3',4,4'-biphenylene tetracarboxylic dianhydride



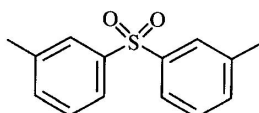
SiDA—bis(3,4-dicarboxyphenyl) dimethylsilane dianhydride



4,4'-ODA—4,4'-oxydianiline



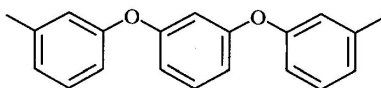
3,3'-ODA—3,3'-oxydianiline



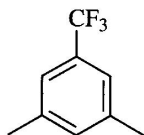
DDSO2—3,3'-diamino diphenylsulfone

(continued)

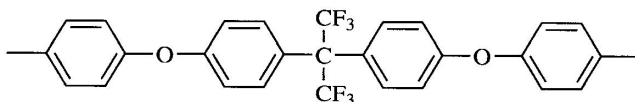
Table 12.1. (continued)



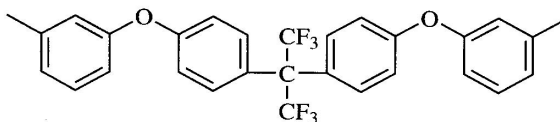
APB—1,3-bis(amino phenoxy)benzene



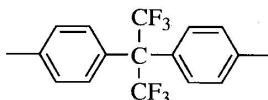
DABTF—3,5-diamino benzotrifluoride



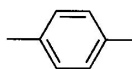
4BDAF—2,2-bis[4(4-aminophenoxy)-phenyl] hexafluoropropane



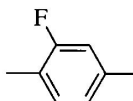
3BDAF—2,2-bis[4(3-aminophenoxy)-phenyl] hexafluoropropane



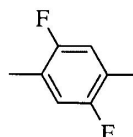
44'6F—2,2-bis(4-aminophenyl) hexafluoropropane)



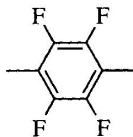
PDA—1,4-diaminobenzene



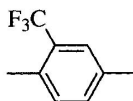
FPDA—1,4-diamino-2-fluorobenzene



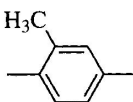
2FPDA—1,4-diamino-2,5-bis-fluorobenzene



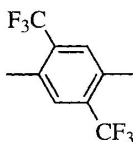
TFPDA—1,4-diaminotetrafluorobenzene



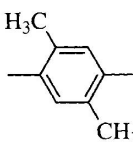
TFMPDA—1,4-diamino-2-(trifluoromethyl)-benzene



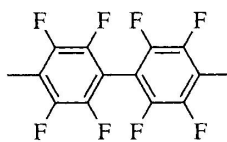
DAT—2,5-diaminotoluene



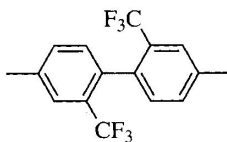
2TFMPDA—1,4-diamino-2,5-bis-(trifluoromethyl)benzene



2DAT—2,5-diamino-4-methyltoluene



OFB—octafluorobenzidine



22' PFMB—2,2' -bis(trifluoromethyl)benzidine

Table 12.2. Comparison of Predicted to Experimental Dielectric Constants

| Polyimide    | Predicted cohesive energy (kJ/mol) | Predicted dielectric constant | Experimental dielectric constant (@10MHz) | Diff. | % Diff. |
|--------------|------------------------------------|-------------------------------|---|-------|---------|
| PMDA+44'ODA  | 167                                | 3.60                          | 3.22                                      | 0.38  | 12      |
| PMDA+33'ODA  | 167                                | 3.60                          | 2.84                                      | 0.76  | 27      |
| BTDA+44'ODA  | 218                                | 3.57                          | 3.15                                      | 0.42  | 13      |
| BTDA+33'ODA  | 218                                | 3.57                          | 3.09                                      | 0.48  | 15      |
| ODPA+44'ODA  | 201                                | 3.48                          | 3.07                                      | 0.41  | 13      |
| ODPA+33'ODA  | 201                                | 3.48                          | 2.99                                      | 0.49  | 16      |
| HQDEA+44'ODA | 235                                | 3.37                          | 3.02                                      | 0.35  | 12      |
| HQDEA+33'ODA | 235                                | 3.37                          | 2.88                                      | 0.49  | 17      |
| BDSDA+44'ODA | 278                                | 3.33                          | 2.97                                      | 0.36  | 12      |
| BDSDA+33'ODA | 279                                | 3.33                          | 2.95                                      | 0.38  | 13      |
| 6FDA+44'ODA  | 221                                | 3.20                          | 2.79                                      | 0.41  | 15      |
| 6FDA+33'ODA  | 221                                | 3.20                          | 2.73                                      | 0.47  | 17      |
| 6FDA+DDSO 2  | 254                                | 3.55                          | 2.86                                      | 0.69  | 24      |
| 6FDA+APB     | 255                                | 3.15                          | 2.67                                      | 0.48  | 18      |
| 6FDA+4BDAF   | 308                                | 2.97                          | 2.50                                      | 0.47  | 19      |
| 6FDA+3BDAF   | 308                                | 2.97                          | 2.40                                      | 0.57  | 24      |
| 6FDA+44'6F   | 240                                | 3.01                          | 2.39                                      | 0.62  | 26      |
| BTDA+DABTF   | 193                                | 3.58                          | 2.90                                      | 0.68  | 23      |
| 6FDA+DABTF   | 196                                | 3.17                          | 2.58                                      | 0.59  | 23      |
| ODPA+DABTF   | 177                                | 3.47                          | 2.91                                      | 0.56  | 19      |
| BPDA+DABTF   | 172                                | 3.44                          | 3.02                                      | 0.42  | 14      |
| SiDA+DABTF   | 184                                | 3.29                          | 2.75                                      | 0.54  | 20      |
| PMDA+4BDAF   | 255                                | 3.14                          | 2.63                                      | 0.51  | 19      |
| BTDA+4BDAF   | 306                                | 3.18                          | 2.74                                      | 0.44  | 16      |
| ODDA+4BDAF   | 289                                | 3.12                          | 2.68                                      | 0.44  | 16      |
| BDSDA+4BDAF  | 366                                | 3.09                          | 2.69                                      | 0.40  | 15      |
| HQDEA+4BDAF  | 323                                | 3.09                          | 2.56                                      | 0.53  | 21      |

samples at a frequency of 10 MHz. The column labeled “Diff” gives the difference between the predicted and the experimental value. The next column gives that difference in percent. This range varies from 12 to 26%. Table 12.3 gives experimental data obtained on dry samples at a frequency of 1 kHz. Predicted Fedors-type cohesive energies are also reported in these tables.

Table 12.4 reports results on the comparison between predicted values of the dielectric constant and experimental values on “wet” samples measured at 1 kHz. Currently the method does not include the effect of moisture (or a frequency dependence of the dielectric constant). It is, however, interesting to see that there is a relatively better correlation between theory and experimental values for the “wet” samples.

Table 12.3. Comparison of Predicted to Experimental Dielectric Constants

| Polyimide    | Cohesive energy density (kJ/mol) | Predicted dielectric constant | Experimental dielectric constant (@1 kHz) | Diff. | % Diff. |
|--------------|----------------------------------|-------------------------------|---|-------|---------|
| 6FDA+PDA     | 187                              | 3.27                          | 2.81                                      | 0.46  | 16      |
| 6FDA+FPDA    | 189                              | 3.25                          | 2.85                                      | 0.40  | 14      |
| 6FDA+2FPDA   | 190                              | 3.23                          | N/A                                       | N/A   | N/A     |
| 6FDA+TFPDA   | 195                              | 3.19                          | 2.68                                      | 0.51  | 19      |
| 6FDA+TFMPDA  | 196                              | 3.17                          | 2.72                                      | 0.45  | 16      |
| 6FDA+DAT     | 191                              | 3.23                          | 2.75                                      | 0.48  | 17      |
| 6FDA+2TFMPDA | 206                              | 3.08                          | 2.59                                      | 0.49  | 19      |
| 6FDA+2DAT    | 195                              | 3.19                          | 2.74                                      | 0.45  | 16      |
| 6FDA+OFB     | 232                              | 3.04                          | 2.55                                      | 0.49  | 19      |
| 6FDA+22'PFMB | 235                              | 3.02                          | 2.72                                      | 0.30  | 11      |

Table 12.4. Comparison of Predicted to Experimental Dielectric Constants of Wet Samples at 1 kHz

| Polyimide    | Predicted dielectric constant | Experimental dielectric constant (@1 kHz) | Diff. | % Diff. |
|--------------|-------------------------------|---|-------|---------|
| 6FDA+PDA     | 3.27                          | 3.22                                      | 0.05  | 1.5     |
| 6FDA+FPDA    | 3.25                          | 3.19                                      | 0.06  | 1.9     |
| 6FDA+2FPDA   | 3.23                          | N/A                                       | N/A   | N/A     |
| 6FDA+TFPDA   | 3.19                          | 3.16                                      | 0.03  | 0.9     |
| 6FDA+TFMPDA  | 3.17                          | 3.05                                      | 0.12  | 3.9     |
| 6FDA+DAT     | 3.23                          | 3.21                                      | 0.02  | 0.6     |
| 6FDA+2TFMPDA | 3.08                          | 2.87                                      | 0.21  | 7.3     |
| 6FDA+2DAT    | 3.19                          | 2.90                                      | 0.29  | 10      |
| 6FDA+OFB     | 3.04                          | 2.73                                      | 0.31  | 11      |
| 6FDA+22'PFMB | 3.02                          | 2.89                                      | 0.13  | 4.5     |

Figure 12.1 shows how well the predicted results agree with the experimental values listed in Table 12.2. The predictions consistently overestimate experimental dielectric constant values for this series of samples. The difference varies from 12 to 27% of the experimental values. Qualitatively, predictions follow the same trend as experiment. The calculated slope for the best straight-line fit through the data points is equal to 0.822 with a standard deviation of 0.088. The correlation coefficient is equal to 0.881. For several of the polyimides tested here the method

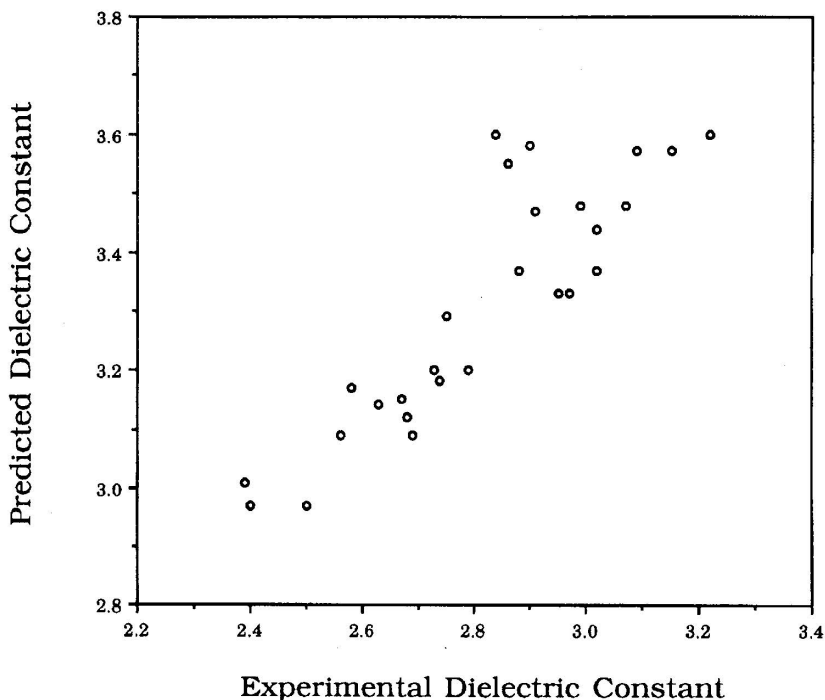


**Figure 12.1.** Comparison of predicted dielectric constants to experimental dielectric constants for a series of dry polyimide samples measured at a frequency of 10 MHz.

produces identical results being unable to distinguish between the para and meta position of the same substituent. See, e.g., the 44' ODA and 33' ODA.

The consistent overestimation of experimental data suggests that the predictions could, in principle, be corrected by subtracting from them a constant number. However, at this stage, the nature of the correction lacks any molecular connection and therefore its use was not warranted.

Figure 12.2 shows the results of comparisons between prediction and experiment for the polyimides listed in Table 12.3. The correlation coefficient is determined to be 0.767. Its value can be improved to 0.957 by not considering the polyimide whose predicted dielectric constant value is equal to 3.02. The slope of the best-fit line is equal to 0.737, with a standard deviation of 0.232.

Figure 12.3 shows results of the comparison for a series of "wet" polyimides at 1 kHz (Table 12.4). The polyimides are the same as the ones shown in Figure 12.2. The main conclusion here is that the bias toward overestimation remains. The correlation coefficient is equal to 0.881, while the slope of the best-fit line is found to be equal to 0.444, with a standard deviation of 0.090.

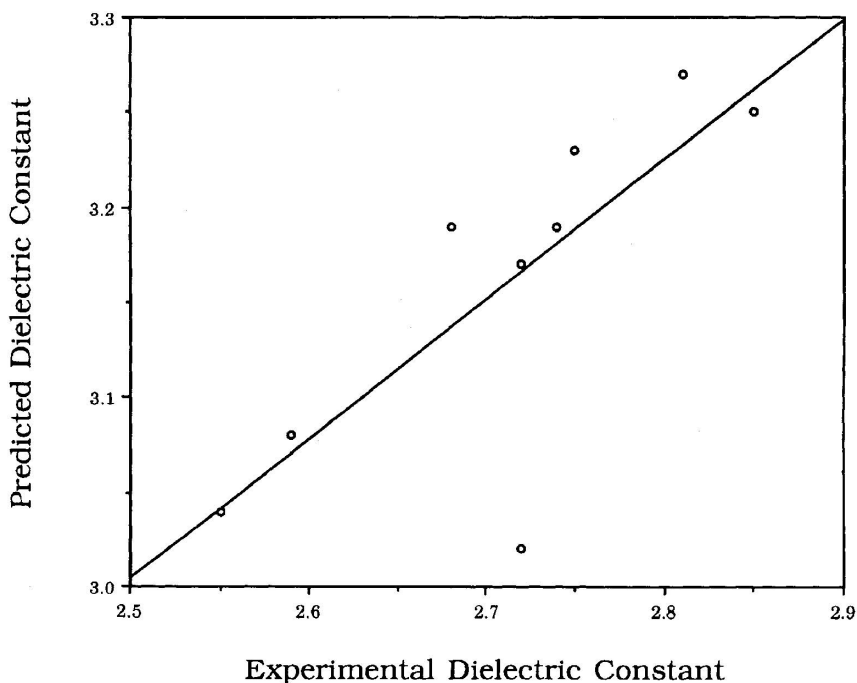


**Figure 12.2.** Comparison of predicted dielectric constants to experimental dielectric constants for a series of dry polyimide samples measured at a frequency of 1 kHz.

## 12.6. CONCLUDING REMARKS

The main advantages of the chemical graph theory are its computational speed, ease of use, and expandability. At this stage, application of chemical graph theory to the prediction of dielectric constants of polyimides yields qualitative results correctly predicting experimental trends. The method seems to always overestimate experimental values. This could be a direct consequence of the fact that Eq. (15) is a result of an extensive database containing many different types of polymers. Polyimides are just one class of those polymers. It is conceivable that the proper choice of a polyimide-specific database might yield quantitative results. This would require the development of a regression equation similar to Eq. (15) but where the correlation is optimized for dielectric constants of typical polyimides. This approach would also include the difference in dielectric constants resulting from meta and para substitutions.

Another important consideration is that all results reported here are based on the calculation of zero- and first-order connectivity indexes only. It is possible that the inclusion of higher-order indexes, which in turn means more detailed

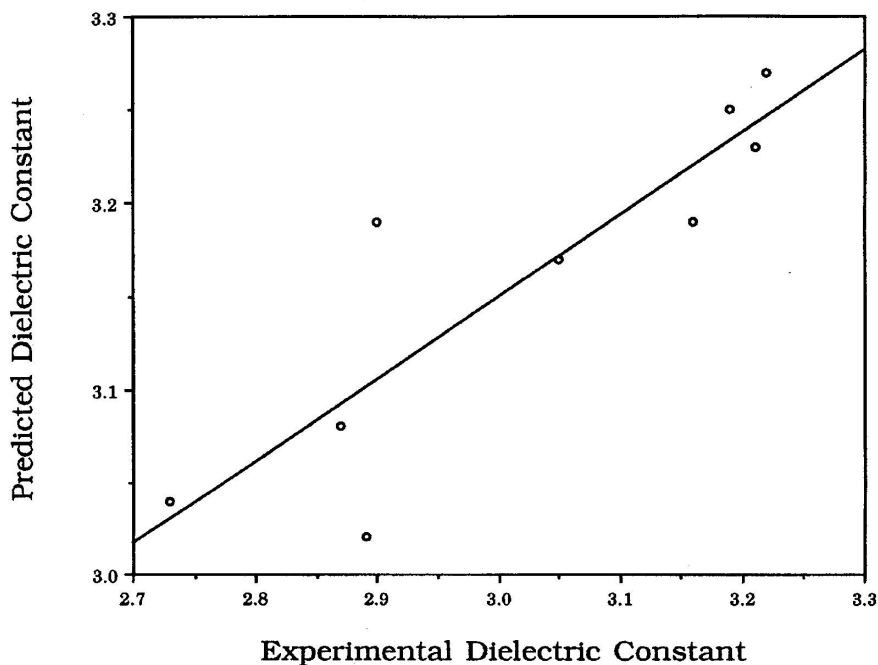


**Figure 12.3.** Comparison of predicted dielectric constants to experimental dielectric constants for a series of wet polyimide samples measured at a frequency of 1 kHz.

connectivity information, might improve the agreement with experiment even further.

Atomistic simulations, even though more time-consuming will also yield valuable information on the dependence of  $\epsilon'$  on chemical structure. One of the advantages of these simulations is that they can, in principle, predict frequency dependence. Work along these lines is in progress.

**ACKNOWLEDGMENTS:** The authors would like to thank Molecular Simulations Inc., for partial support.

## 12.7. REFERENCES

1. D. W. van Krevelen, *Properties of Polymers, 3rd Ed.* Elsevier, Amsterdam (1993).
2. D. W. van Krevelen, in *Computational Modeling of Polymers* (J. Bicerano, ed.), Marcel Dekker, New York (1992).
3. W. Klonowski, *Mater. Chem. Phys.* 14, 581 (1986).
4. J. W. Kennedy, *Anal. Chem. Symp. Ser. (Comp. Appl. Chem.)* 15, 151 (1983).



5. J. Bicerano, *Prediction of Polymer Properties*, Marcel Dekker, New York (1993).
6. V. Galiatsatos, E. S. Castner, and A. M. S. Al-ghamdi, *Makromol. Chem.—Macromolecular Symp.* 93, 155 (1995).
7. E. S. Castner and V. Galiatsatos, *Comput. Polym. Sci.* 4, 41 (1994).
8. V. Galiatsatos, *Polym. Eng. Sci.* 33, 285 (1993).
9. V. Galiatsatos and B. Eichinger, *Rubber Chem. Tech.* 61, 205 (1988).
10. V. Galiatsatos and B. Eichinger, *J. Polym. Sci. Pt. B: Polym. Phys.* 26, 595 (1988).
11. L. B. Kier and L. H. Hall, *Molecular Connectivity in Structure-Activity Analysis*, John Wiley and Sons, New York (1986).
12. L. B. Kier and L. H. Hall, *Molecular Connectivity in Chemistry and Drug Research*, Academic Press, New York (1976).
13. A. J. Polak and R. C. Sundahl, *Polym. Eng. Sci.* 14, 147 (1974).
14. R. F. Fedors, *Polym. Eng. Sci.* 14, 147 (1974).
15. A. K. St. Clair, T. L. St. Clair, and W. P. Winfree, *PMSE Preprints*, ACS 59, 28 (1988).
16. G. G. Hougham, G. Tesoro, and J. Shaw, *Macromolecules* 27, 3642 (1994).
17. D. M. Stoakley, A. K. St. Clair, and R. M. Baucom, *SAMPE Quart.* 21, 3 (1989).
18. M. K. Gerber, J. R. Pratt, and A. K. St. Clair, *Polym. Preprints* 31, 340 (1990).